20. Hosoyamada M, Yan K, Nishibori Y *et al*. Nephrin and podocin expression around the onset of puromycin aminonucleoside nephrosis. *J Pharmacol Sci* 2005; 97: 234–241
21. Peraldi MN, Morelon E, Mamzer-Brunel MF *et al*. Renal function and pathology after switch from calcineurin-dependent drugs to sirolimus in renal transplant recipients with chronic graft nephropathy [abstract A3694]. *J Am Soc Nephrol* 2000; 11: 702A
22. Daniel C, Renders L, Amann K *et al*. Mechanisms of everolimus-induced glomerulosclerosis after glomerular injury in the rat. *Am J Transplant* 2005; 5: 2849–2861
23. Schrijvers BF, Flyvbjerg A, De Vriese AS. The role of vascular endothelial growth (VEGF) in renal pathophysiology. *Kidney Int* 2004; 65: 2003–2017
24. Diekmann F, Rovira J, Carreras J *et al*. Mammalian target of rapamycin inhibition halts the progression of proteinuria in a rat model of reduced renal mass. *J Am Soc Nephrol* 2007; 18: 2653–2660
25. Vogelbacher R, Wittmann S, Braun A *et al*. The mTOR inhibitor everolimus induces proteinuria and renal deterioration in the remnant kidney model in the rat. *Transplantation* 2007; 84: 1492–1499
26. Liu G, Kaw B, Kurfis J *et al*. Neph1 and nephrin interaction in the slit diaphragm is an important determinant of glomerular permeability. *J Clin Invest* 2003; 112: 209–221
27. Zhu J, Sun N, Aoudjit L *et al*. Nephrin mediates actin reorganization via phosphoinositide 3-kinase in podocytes. *Kidney Int* 2008; 73: 524–526
28. Hostetter TH, Olson JL, Rennke HG *et al*. Hyperfiltration in remnant nephrons: a potentially adverse response to renal ablation. *J Am Soc Nephrol* 2001; 12: 1315–1325
29. Rodriguez-Iturbe B, Vaziri ND, Herrera-Acosta J *et al*. Oxidative stress, renal infiltration of immune cells, and salt-sensitive hypertension: all for one and one for all. *Am J Physiol Renal Physiol* 2004; 286: F606–F616
30. Chow F, Ozols E, Nikolic-Paterson DJ *et al*. Macrophages in mouse type 2 diabetic nephropathy: correlation with diabetic state and progressive renal injury. *Kidney Int* 2004; 65: 116–128
31. Fujihara CK, Antunes GR, Mattar AL *et al*. Cyclooxygenase-2 (COX-2) inhibition limits abnormal COX-2 expression and progressive injury in the remnant kidney. *Kidney Int* 2003; 64: 2172–2181
32. Anders HJ, Ninichuk V, Schlondorff D. Progression of kidney disease: blocking leukocyte recruitment with chemokine receptor CCR1 antagonists. *Kidney Int* 2006; 69: 29–32
33. Herrero-Fresneda I, Torras J, Vidal A *et al*. Reduction of postischemic immune inflammatory response: an effective strategy for attenuating chronic allograft nephropathy. *Transplantation* 2005; 79: 165–173
34. Fornoni A, Ijaz A, Tejada T *et al*. Role of inflammation in diabetic nephropathy. *Curr Diabetes Rev* 2008; 4: 10–17
35. Rastaldi MP. Epithelial-mesenchymal transition and its implications for the development of renal tubulointerstitial fibrosis. *J Nephrol* 2006; 19: 407–412
36. Herrero-Fresneda I, Torras J, Franquesa M *et al*. HGF gene therapy attenuates renal allograft scarring by preventing the profibrotic inflammatory-induced mechanisms. *Kidney Int* 2006; 70: 265–274
37. Wu MJ, Wen M, Chiu Y *et al*. Rapamycin attenuates unilateral ureteral obstruction-induced renal fibrosis. *Kidney Int* 2006; 69: 2029–2036
38. Jain S, Bicknell GR, Whiting PH *et al*. Sirolimus reduces expression of fibrosis-associated genes in an experimental model of renal ischemia reperfusion injury. *Transplant Proc* 2001; 33: 556–558
39. Kim YH, Goyal M, Kurnit D *et al*. Podocyte depletion and glomerulosclerosis have a direct relationship in the PAN-treated rat. *Kidney Int* 2001; 60: 957–968
40. Coombes JD, Mreich E, Liddle C *et al*. Rapamycin worsens renal function and intratubular cast formation in protein overload nephropathy. *Kidney Int* 2005; 68: 2599–2607
41. Yang X, Shen Y, Zhu Z *et al*. Apoptosis signaling pathway in a subtotal nephrectomy rat model. *J Huazhong Univ Sci Technolog Med Sci* 2006; 26: 425–428
42. Nagai K, Matsubara T, Mima A *et al*. Gas6 induces Akt/mTOR-mediated mesangial hypertrophy in diabetic nephropathy. *Kidney Int* 2005; 68: 552–561
43. Sarbassov DD, Guertin DA, Ali SM *et al*. Phosphorylation and regulation of Akt/PKB by the rictor-mTOR complex. *Science* 2005; 307: 1098–1101
44. Zeng Z, Sarbassov dos D, Samudio IJ *et al*. Rapamycin derivatives reduce mTORC2 signaling and inhibit AKT activation in AML. *Blood* 2007; 109: 3509–3512

Received for publication: 4.12.08; Accepted in revised form: 1.7.09

Nephrol Dial Transplant (2009) 24: 3640–3651
doi: 10.1093/ndt/gfp371
Advance Access publication 8 August 2009

Increased renoprotection with ACE inhibitor plus aldosterone antagonist as compared to monotherapies—the effect on podocytes

Zalan Nemeth[1,*], Gabor Kokeny[1,2,*], Maria Godo[1], Miklós Mózes[1], László Rosivall[1], Marie-Luise Gross[2], Eberhard Ritz[3] and Péter Hamar[1]

[1]Department of Pathophysiology, Semmelweis University, Budapest, Hungary, [2]Institute of Pathology and [3]Department of Internal Medicine, University of Heidelberg, Heidelberg, Germany

Correspondence and offprint requests to: Péter Hamar; E-mail: hampet@net.sote.hu

*The first two authors contributed equally to this work.

Abstract

Background. Blockade of the renin–angiotensin–aldosterone system (RAAS) does not completely prevent progression of renal disease. Mineralocorticoid receptor blockade provides additional renoprotection over ACE-inhibition monotherapy. We examined the mechanisms

© The Author 2009. Published by Oxford University Press [on behalf of ERA-EDTA]. All rights reserved.
For Permissions, please e-mail: journals.permissions@oxfordjournals.org

Downloaded from ndt.oxfordjournals.org at Semmelweis University Medicine on April 15, 2011

underlying superior renoprotection in the subtotal nephrectomy (SNX) model.

Methods. Sprague-Dawley rats were randomized into six groups: (1) sham-op, (2) SNX without treatment, (3) SNX + quinapril (Q), (4) SNX + spironolactone (S), (5) SNX + combination therapy (Q+S), (6) SNX + combination hydrochlorothiazide + reserpin + hydralazine (HRH). Albuminuria and blood pressure were monitored, and kidneys were examined by morphometric and molecular methods.

Results. In SNX rats, albumin excretion was significantly higher than in sham-op rats. Blood pressure reduction was not significantly different between the treatment groups. All therapies (S, Q, Q+S and HRH) reduced albuminuria; the values were lowest in animals treated with Q+S. The volume density of glomerular matrix and the number of mesangial cells were significantly increased in SNX and were lowest in SNX treated with Q+S. The number of podocytes was reduced in SNX, but was normalized in SNX treated with Q+S. Glomerular volumes and podocyte volumes were significantly higher in SNX than in sham-op. Both volumes were reduced by all interventions, but almost normalized by treatment with Q+S. Expression of collagen IV, TGF-β_1 and desmin was increased after SNX and significantly reduced by treatment with Q and Q+S.

Conclusions. In subtotally nephrectomized rats, mineralocorticoid blockade provided additional renoprotection over and above ACE inhibition. Such benefit was paralleled by major changes in podocyte number and morphology and was not blood pressure dependent.

Keywords: aldosterone; chronic kidney failure; progression of chronic renal failure; renin–angiotensin system

Introduction

Progressive renal fibrosis is the common final pathway of many kidney diseases [1,2]. The renin–angiotensin system (RAS) plays an important role in this process and RAS blockade ameliorates progression of renal fibrosis.

Besides the systemic RAS, local RAS operate independent of the systemic RAS [3,4] in the kidney, i.e. in proximal tubular cells, podocytes and mesangial cells [5,6]. In animal experiments, administration of an ACE inhibitor results in almost complete inhibition of systemic angiotensin II (ANG II) formation, while it has little or no effect on intrarenal ANG II production [7]. There is also evidence that ANG II can be produced by alternative enzymes such as chymases [8] that cannot be blocked by ACE inhibitor treatment and that alternative ANG II producing pathways are stimulated during systemic ACE inhibition [9]. These alternative pathways of intrarenal ANG II production may explain in part why even high doses of angiotensin-converting enzyme (ACE) inhibitors alone cannot completely prevent progressive renal damage. An alternative possibility is a progressivie increase in aldosterone production, presumably caused by non-ACE-dependent ANG II formation with subsequent induction of aldosterone synthesis [10].

The role of aldosterone in the progression of renal disease has recently attracted considerable attention. There is evidence that aldosterone has direct effects on renal cells, independent of ANG II, which contribute to progression of renal disease [11,12]. Hostetter and collegues showed that aldosterone directly upregulates expression of the profibrotic factor TGF-β_1 in the kidney [12]. Aldosterone also upregulates the expression of plasminogen activator inhibitor-1 (PAI-1) [13], which would favour fibrosis in renal structures, and induces collagen IV synthesis of mesangial cells *in vitro* [14] as well as expression of connective tissue growth factor (CTGF) and endothelin-1 [14]. Conversely, however, in the classical rat remnant kidney model, aldosterone inhibition with spironolactone ameliorated proteinuria, but had no effect on glomerulosclerosis [15].

In order to provide optimal renoprotection, a multidrug approach has been proposed as appropriate [16], although this may be difficult to prove in controlled prospective studies [2,17]. However, there is some clinical [18] evidence pointing in this direction and also some evidence in experimental renal damage models with proteinuria [19–21].

In the current study, we compared in the renal ablation model the effects of monotherapy with an ACE inhibitor (quinapril), mineralocorticoid receptor blocker (spironolactone) and their combination with antihypertensive triple therapy without specific effects on the RAS as controls. The readouts were proteinuria, quantitative renal morphology and the expression of molecules relevant in progression.

Methods

Experimental design and operative procedures

Twenty-week old male Sprague-Dawley (SD) rats weighing 350–400 g were used (Charles River, Germany). All animals were housed under standard conditions (light on 08:00–20:00 h; 40–70% relative humidity, $22 \pm 1^{\circ}$C), and had free access to water and chow (Altromin standard diet, Lage, Germany). All procedures were in accordance with the guidelines of the German Institutional Animal Care and Use Committee. The animals were subjected randomly to subtotal nephrectomy (SNX) ($n = 56$) or sham operation (sham-op) ($n = 12$). The SNX animals were randomly divided into six groups: (1) sham-op, (2) SNX untreated ($n = 12$/group); (3) SNX + quinapril (SNX+Q) ($n = 12$/group); (4) SNX + spironolactone (SNX+S) ($n = 12$/group); (5) SNX + combination quinapril + spironolactone (SNX+Q+S) ($n = 12$/group); (6) SNX + hydrochlorothiazide + reserpin + hydralazine (SNX+HRH) ($n = 8$/group). Sham-op animals were observed as controls.

The quinapril dose (Quinapril-HCT Hexal, Hexal, Germany) was 50 mg/kg body weight/day, the Spironolactone dose (as water soluble potassium canrenoate Aldactone, Roche, Germany) 10 mg/kg body weight and antihypertensive triple therapy hydrochlorothiazide, reserpine and hydralazine were 1.25 mg/kg, 0.25 mg/kg and 4 mg/kg, respectively. All medications were dissolved and applied in drinking water adjusting the drug concentration according to fluid consumption. The untreated sham-op and untretaed SNX received tap water. The duration of the experiment was 12 weeks.

SNX was performed as described [22]. In brief, under isoflurane anaesthesia (Baxter, Germany), the animals were uninephrectomized, i.e. the right kidney was decapsulated and removed. One week later, two-third of the decapsulated left kidney was removed by resecting a specified amount of cortical tissue, leaving the pelvis and the hilus intact. Damage to the adrenals at decapsulation was carefully avoided. Tabotamp® (Ethicon, Switzerland) was used for haemostasis. The excised renal tissue was weighed on an analytic scale. In sham-op animals, the kidneys were only decapsulated.

Downloaded from ndt.oxfordjournals.org at Semmelweis University Medicine on April 15, 2011

Functional measurements

Two and 3 months after surgery, 24-h urine was collected using metabolic cages (Tecniplast, Buguggiate, Italy). At the end of the study, tail-cuff blood pressure was measured in conscious animals by electrosphygmomanometry in conscious rats (TSE GmbH., Bad Homburg, Germany) [23]. Urinary albumin excretion was determined using a microplate sandwich ELISA [24] modified by using a rabbit anti-rat albumin peroxidase conjugate. Blood urea nitrogen and serum creatinine levels were evaluated in a Reflotron Plus laboratory machine with enzymatic reagents (Boehringer, Mannheim, Germany).

Tissue preparation

Retrograde perfusion fixation of the kidney with 3% glutaraldehyde was performed via the abdominal aorta [25]. The left remnants (or in sham-op animals the left kidneys) were harvested for morphometric and stereologic measurements. The kidneys were sectioned in a plane perpendicular to the interpolar axis, yielding slices of 1 mm width. Ten small pieces of the kidney were selected by area-weighted sampling and embedded in Epon-Araldite. Semithin (1 μm) sections were prepared and stained with methylene blue/basic fuchsine. The remaining tissue slices were embedded in paraffin; 4 μm sections were stained with haematoxylin/eosin (HE) and periodic acid-Schiff (PAS).

For immunohistochemical analysis, the experiment was repeated and terminated perfusing the kidney with ice-cold NaCl ($n = 9$/group). One-half of the saline-perfused kidneys were immersion fixed in 4% buffered formaldehyde, embedded in paraffin and cut into 4 μm thick sections, the other half were snap frozen in liquid nitrogen for real-time PCR analysis.

Morphological and stereological evaluation

All investigations were performed in a blinded manner, i.e. the observer was unaware of the study group the animal belonged to.

Glomerular damage indices. The glomerulosclerosis index was assessed on PAS-stained paraffin sections according to the scoring system (scores: 0–4) of El Nahas *et al*. [26]. The glomerular score of each animal was derived as the arithmetic mean of 100 glomeruli using light microscopy and a magnification of ×400. The tubular, interstitial and vascular damage scores were assessed on PAS-stained paraffin sections using a similar scoring system (score 0–4) at a magnification of ×100 as described in detail elsewhere [27].

Glomerular geometry. The area density of the glomerular tuft (A_{AT}) and the volume density of glomeruli (V_V) were measured by the point counting method with point density = area density = volume density ($P_P = A_A = V_V$) using a 100-point Zeiss eyepiece (Integration-plate II; Zeiss Co., Oberkochen, Germany) at a magnification of ×400 on the PAS sections. In addition, the number of glomeruli per area (N_A) was counted. For detailed description of analysis of glomerular geometry see [28]. Briefly, from the above data, the number of glomeruli per volume [$N_V = (1/1.382) \times (N_A{}^{1.5} \times V_V{}^{0.5})$] (corrected for tissue shrinkage: 45%) and total cortex volume was calculated from kidney mass (KW), specific weight of the kidney (SW_K) and volume density of the cortex according to $V_{Cortex} = KW/SW_K \times V_{VCortex}$ (V_{Cortex}) $= (1/1.382) \times (N_A{}^{1.5} \times V_V{}^{0.5})$. From these parameters, the total number of glomeruli was derived ($N_{Glom} = N_V \times V_{Cortex}$). Finally, the mean glomerular tuft volume ($mV_{Glom} = (1/1.382) \times A_T{}^{1.5}$) was calculated from the total area of the glomerular tuft and the cortex area ($A_T = A_{AT} \times A_{cortex}$). The number of glomeruli (N_{Glom}) per kidney was used to estimate the extent of surgical nephron reduction, and the mean glomerular tuft volume (mV_{Glom}) was used to estimate the extent of glomerular enlargement. The glomerular mesangial matrix volume (V_{Matrix}) was calculated as the fractional mesangial matrix volume of the glomerular capillary tuft (points on the matrix/points on the whole glomerular tuft) and is given as percent.

Glomerular capillaries. In five semithin sections per animal, glomerular cell number and volume were analysed using an eyepiece for point counting (see above) at a magnification of ×1000 (oil immersion). Briefly, the length density of glomerular capillaries (L_V: mm capillary/mm^3 glomerular tuft volume) was determined according to the standard stereologic formula ($L_V = 2Q_A$: the number of capillary transects per area of the capillary tuft). This parameter gives the average capillary length normalized to glomerular volume—excluding the effect of hypertrophy; thus it is a marker of glomerular capillary obliteration [28]. Furthermore, the glomerular capillary length for the whole kidney (L_c), i.e. total capillary length, was determined. The glomerular capillary tuft volume (V_{Tuft}) was calculated as the fractional capillary tuft volume of the whole glomerulus (points on the tuft/points on the whole glomerulus) and is given as percent.

Glomerular cellularity. The number per glomerulus and the mean volume of glomerular cells (podocytes, mesangial and endothelial cells) were analysed in 15 glomeruli per animal. The mean cell number/glomerulus (N_C) was calculated from the cell density per volume (Nc_V) and the volume density of the respective cell type (Vc_V) according to the equation: $Nc_V = \kappa/\beta \times Nc_A{}^{1.5}/Vc_V{}^{0.5}$ with $\kappa = 1$ and $\beta = 1.5$ for podocytes and 1.4 for mesangial and endothelial cells. The respective mean cell volumes were calculated according to the equation $mV_c = Vc_V \times V_{glom}$ [29].

Immunohistochemistry

Paraffin sections were prepared and incubated with antibodies, using the avidin–biotin method [30], to detect desmin (anti-desmin monoclonal mouse antibody, 1:50; DAKO), fibronectin (anti-fibronectin rabbit polyclonal antibody, 1:1000; Sigma, Germany), TGF-β_1 (anti- TGF-β_1 rabbit polyclonal antibody, 1:100; Santa Cruz) and collagen IV (anti-collagen IV rabbit polyclonal antibody, 1:40, Biotrend Chemicalien GmbH, Cologne, Germany). Immunohistochemical reactivity was examined with light microscopy at a magnification of ×400. Semiquantitative scoring (scores 0–4; 0: no staining, 1: weak, 2: mild, 3: strong, 4: very strong staining) was performed as described elsewhere [31].

Real-time PCR

Total RNA was isolated from kidney tissue using the SV Total RNA Isolation System (Promega, Mannheim, Germany) according to the manufacturer's instructions. RNA concentration was determined photometrically.

Reverse transcription was performed with the First Strand cDNA Synthesis Kit (AMV) from Roche (Roche Diagnostics, Mannheim, Germany) using 1 μg RNA and random primers (final concentration: 3.2 μg).

All PCR reactions were performed on a LightCycler (Roche Diagnostics) using the LighCycler-Faststart DNA Master SYBR Green I Kit (Roche). The samples were quantified normalizing to glyceraldehyde-3-phosphate dehydrogenase (GAPDH) expression. Primer sequences for TGF-β_1 were as follows: forward 5′-CACCATCCATGACATGAACC-3′, reverse 5′-TCATGTTGGACAACTGCTCC-3′. Specificity of the PCR reaction was confirmed with melting curve analysis. Every sample was quantified using a gene-specific standard curve, and the mean value of three different PCR runs was taken for statistical evaluation.

Statistics

Data are presented as mean ± SD. ANOVA followed by the Tukey *post hoc* test and the Kruskal–Wallis test followed by Dunn's test were used to compare the groups.

Results

Animal data (Table 1)

The average body weight was similar in all groups initially and at the end of the study. Although no pair-feeding protocol was used, measured food consumption and body weight gain were not different between the groups.

The weight of the remnant kidney in all SNX groups was greater than that of the left kidney in the sham group. Remnant kidney hypertrophy was reduced by quinapril and combination treatment (quinapril + spironolactone: Q+S), but not by spironolactone monotherapy or by triple therapy (hydrochlorothiazide + reserpin + hydralazine: HRH).

The reduction of haematocrit was not significantly affected by any of the treatments. At the end of the study, the Htk was similarly reduced in all treatment groups compared to sham-op.

Downloaded from ndt.oxfordjournals.org at Semmelweis University Medicine on April 15, 2011

Table 1. Body weight, kidney weight and laboratory values

Groups	Initial body weight (g)	Body weight at harvest (g)	Left kidney weight (g)	Haematocrit (%)	Blood Urea (mg/dl)	Se Crea (mg/dl)
Sham ($n = 12$/group)	239.2 ± 8.6	557 ± 37	1.78 ± 0.12	43.2 ± 3.4	41.7 ± 7.5	0.46 ± 0.05
SNX ($n = 12$/group)	236.0 ± 5.5	574 ± 54	2.46 ± 0.23*	34.8 ± 6.3*	122 ± 47.3*	0.85 ± 0.13*
SNX + Q ($n = 12$/group)	236.7 ± 5.8	554 ± 77	1.95 ± 0.28#,&	39.3 ± 3.4	90.5 ± 15.4*,#	0.75 ± 0.06*
SNX + S ($n = 12$/group)	236.0 ± 4.2	542 ± 44	2.43 ± 0.18*	38.3 ± 5.4	94.4 ± 20.4*	0.78 ± 0.07*
SNX + Q + S ($n = 12$/group)	243.8 ± 2.5	540 ± 44	2.07 ± 0.22#,&	38.6 ± 5.3	85.7 ± 17.7*,#	0.63 ± 0.07*,#,&,$
SNX + HRH ($n = 8$/group)	238.5 ± 8.9	526 ± 36	2.52 ± 0.50*	nd	86.3 ± 10.1*,#	0.68 ± 0.05*,#,&,$
ANOVA	ns	ns	$P < 0.0001$	$P < 0.05$	$P < 0.0001$	$P < 0.0001$

*$P < 0.05$ versus sham, #$P < 0.05$ versus SNX, &$P < 0.05$ versus SNX+S, $$P < 0.05$ versus SNX+Q.
Q, quinapril; S, spironolactone; HRH, hydrochlorothiazide+reserpin+hydralazine.
Data as mean ± SD.

Blood urea and creatinine concentrations were significantly elevated in all SNX groups compared to sham-op. Q, Q+S and HRH reduced urea concentrations, but creatinine was significantly lower only in Q+S and HRH.

Albuminuria and blood pressure (Table 2)

In untreated SNX, albumin excretion increased progressively from 2 to 3 months after operation. At 2 months, albumin excretion was lower in the Q and HRH groups, but was lowest in the combination (Q+S) treatment group. At 3 months, albuminuria had doubled in SNX, but remained low in Q-, S- and HRH-treated animals. The Q+S combination lowered albuminuria more effectively than Q, S or HRH.

In SNX, blood pressure was elevated 3 months after operation compared to sham-op. Both Q+S and HRH combination therapies and Q monotherapy normalized blood pressure, whereas monotherapy with S was less effective.

Indices of renal damage (Figure 1, Table 3)

In SNX animals, the *glomerulosclerosis index* was reduced in all groups treated with Q; of note, combination treatment (Q+S) was more effective than Q monotherapy.

The tubulointerstitial damage index was lower in all treatment groups, but was lowest in rats on the combination Q+S.

The *vascular damage index* was lower in SNX animals treated with Q and Q+S, but not in animals treated with monotherapy or the HRH combination.

The glomerular mesangial matrix volume was increased 2.5 fold in untreated SNX compared to sham-op. All treatments (S, Q, S+Q, HRH) reduced mesangial matrix deposition, but the combination Q+S was the most effective.

Glomerulus geometry and glomerular capillaries (Table 4)

The reduction of the number of glomeruli by SNX was similar, documenting uniformity of the resection of renal parenchyma.

In all SNX groups, a compensatory increase in glomerular volume was present. Glomerular hypertrophy was significantly less in animals with Q and Q+S treatment. Treatment with S and HRH had no effect.

The length density of glomerular capillaries was significantly less in SNX reflecting capillary loss or obliteration as a result of glomerulosclerosis. Both Q and Q+S reduced capillary loss to a similar extent, but S monotherapy and HRH had no significant effect.

Cellular analysis of the glomeruli (Table 5)

The number of podocytes per glomerulus was markedly reduced in untreated SNX compared to sham, and podocyte volume increased strikingly. Compared to SNX alone, podocyte hypertrophy was reduced in all treatment groups. However, only the anti-renin–angiotensin–aldosterone system (RAAS) combination treatment (Q+S) was able to reduce podocyte volume to a level not significantly differing from sham-op controls. In SNX animals, podocyte loss was documented with a significant reduction in podocyte number compared to sham-op. Podocyte loss was reduced by monotherapies, and prevented by anti-RAAS combination treatment.

The number of endothelial cells were also strikingly higher in untreated SNX compared to sham-op. Endothelial cell proliferation was significantly reduced by quinapril and combination treatment, but not by spironolactone. Endothelial cell volume was not affected by SNX or therapy.

Similarly, mesangial cell number was significantly elevated in untreated SNX. Spironolactone and HRH treatment reduced mesangial proliferation. However, quinapril monotherapy was more effective than HRH, but only anti-RAAS combination treatment reduced mesangial proliferation to the level of sham-op animals. Mesangial cell volume was not significantly influenced by SNX.

Immunohistochemical and RT-PCR analysis (Tables 6 and 7)

Glomerular *desmin* staining, a marker of podocyte damage, was markedly more intense in untreated SNX compared to sham (Figure 2). Only quinapril and anti-RAAS combination treatment reduced desmin staining significantly. But anti-RAAS combination treatment was the most effective to prevent podocyte damage.

Glomerular and the tubulointerstitial *collagen IV* staining was significantly more intense (Figure 3) in untreated SNX compared to sham. Staining tended to be less

Downloaded from ndt.oxfordjournals.org at Semmelweis University Medicine on April 15, 2011

Table 2. Albuminuria and Blood pressure

Groups	Albuminuria 2 months post-OP (mg/day)	Albuminuria 3 months post-OP (mg/day)	MABP 3 months post-OP (mmHg)
Sham ($n = 10$/group)	0.7 ± 0.6	1.4 ± 0.8	97 ± 8
SNX ($n = 10$/group)	$27.8 \pm 8.8^{*}$	$59.3 \pm 18.1^{*}$	$127 \pm 7^{*}$
SNX + Q ($n = 10$/group)	$13.1 \pm 2.3^{*,\#}$	$13.1 \pm 11.8^{*,\#}$	$93 \pm 13^{\#}$
SNX + S ($n = 10$/group)	$18.2 \pm 5.1^{*}$	$26.7 \pm 14.3^{*,\#}$	$107 \pm 7^{*}$
SNX + Q + S ($n = 10$/group)	$3.8 \pm 2.1^{*,\#,\&,\$}$	$7.1 \pm 3.3^{*,\#,\&,\$,\S}$	$94 \pm 6^{\#}$
SNX + HRH ($n = 6$/group)	$7.5 \pm 9.6^{*,\#,\&}$	$27.4 \pm 15.7^{*,\#}$	$96 \pm 6^{\#}$
ANOVA	$P < 0.0001$	$P < 0.0001$	$P < 0.0001$

$^{*}P < 0.05$ versus sham, $^{\#}P < 0.05$ versus SNX, $^{\&}P < 0.05$ versus SNX+S, $^{\$}P < 0.05$ versus SNX+Q, $^{\S}P < 0.05$ versus SNX+HRH.
MABP, mean arterial blood pressure; Q, quinapril; S, spironolactone; HRH, hydrochlorothiazide+reserpin+hydralazine.
Data as mean ± SD.

Table 3. Morphologic indices of renal damage

Groups	Glomerulosclerosis index	Tubulointerstitial damage index	Vascular damage index	Volume of mesangial matrix (V_{matrix},%)
Sham ($n = 10$/group)	0.14 ± 0.07	0.20 ± 0.14	0.06 ± 0.04	7.6 ± 2.8
SNX ($n = 10$/group)	$1.72 \pm 0.48^{*}$	$2.19 \pm 0.56^{*}$	$1.43 \pm 0.14^{*}$	$24.6 \pm 3.9^{*}$
SNX + Q ($n = 10$/group)	$1.03 \pm 0.20^{*,\#}$	$1.15 \pm 0.43^{*,\#}$	$0.66 \pm 0.49^{*,\#,\&}$	$13.9 \pm 2.4^{*,\#}$
SNX + S ($n = 10$/group)	$1.31 \pm 0.20^{*}$	$1.45 \pm 0.28^{*,\#}$	$1.43 \pm 0.28^{*}$	$19.1 \pm 2.8^{*,\#}$
SNX + Q + S ($n = 10$/group)	$0.69 \pm 0.21^{\#,\&,\$}$	$0.76 \pm 0.25^{\#,\&,\$}$	$0.63 \pm 0.29^{*,\#,\&}$	$9.4 \pm 2.1^{\#,\&,\$}$
SNX + HRH ($n = 6$/group)	$1.20 \pm 0.14^{*}$	$1.31 \pm 0.24^{*,\#}$	$1.35 \pm 0.36^{*}$	$18.1 \pm 5.7^{*,\#}$
ANOVA	$P < 0.0001$	$P < 0.0001$	$P < 0.0001$	$P < 0.0001$

$^{*}P < 0.05$ versus sham, $^{\#}P < 0.05$ versus SNX, $^{\&}P < 0.05$ versus SNX+S, $^{\$}P < 0.05$ versus SNX+HRH.
Q, quinapril, S, spironolactone; HRH, hydrochlorothiazide+reserpin+hydralazine.
Data as mean ± SD.

Table 4. Glomeruli: number, size and capillaries

Groups	Glomeruli number/kidney	Mean glomerular volume ($[\times 10^{6}\ \mu m^{3}$)	Length density (mm/mm^{3})	Total length (mm)
Sham ($n = 8$/group)	$63\,703 \pm 12\,663$	1.09 ± 0.13	9.1 ± 1.7	$21\,141 \pm 7909$
SNX ($n = 8$/group)	$24\,881 \pm 7208^{*}$	$3.23 \pm 0.63^{*}$	$4.8 \pm 0.9^{*}$	$8267 \pm 804^{*}$
SNX + Q ($n = 8$/group)	$29\,229 \pm 4443^{*}$	$2.44 \pm 0.08^{*,\#}$	$6.6 \pm 0.3^{*}$	$11\,353 \pm 2895^{*}$
SNX + S ($n = 8$/group)	$23\,555 \pm 9050^{*}$	$2.73 \pm 0.44^{*}$	$5.8 \pm 1.3^{*}$	$7502 \pm 2047^{*}$
SNX + Q + S ($n = 8$/group)	$23\,737 \pm 3790^{*}$	$1.81 \pm 0.21^{*,\#,\&,\$}$	$7.3 \pm 2.1^{*,\#}$	$9748 \pm 2698^{*}$
SNX + HRH ($n = 8$/group)	$26\,657 \pm 2902^{*}$	$2.61 \pm 0.37^{*}$	$4.8 \pm 0.8^{*}$	$9915 \pm 2163^{*}$
ANOVA	$P < 0.0001$	$P < 0.0001$	$P < 0.0001$	$P < 0.0001$

$^{*}P < 0.05$ versus sham, $^{\#}P < 0.05$ versus SNX, $^{\&}P < 0.05$ versus SNX+S., $^{\$}P < 0.05$ versus SNX+HRH.
Q, quinapril; S, spironolactone; HRH, hydrochlorothiazide+reserpin+hydralazine.
Data as mean ± SD.

Table 5. Cellular analysis of the glomerulus

	Endothelial cells		Mesangial cells		Podocytes	
Groups	Number/ glomerulus	volvo Mean volume (μm^{3})	Number/ glomerulus	volvo Mean volume (μm^{3})	Number/ glomerulus	volvo Mean volume (μm^{3})
Sham ($n = 8$/group)	602 ± 122	53 ± 12	360 ± 66	52 ± 8	183 ± 28	375 ± 113
SNX ($n = 8$/group)	$1354 \pm 370^{*}$	42 ± 12	$1231 \pm 220^{*}$	47 ± 15	$127 \pm 14^{*}$	$1620 \pm 360^{*}$
SNX + Q ($n = 8$/group)	$773 \pm 139^{\#,\&}$	56 ± 15	$752 \pm 62^{*,\#}$	53 ± 13	152 ± 7	$951 \pm 213^{*,\#}$
SNX + S ($n = 8$/group)	$1335 \pm 499^{*}$	49 ± 10	$929 \pm 172^{*,\#}$	45 ± 9	154 ± 35	$1177 \pm 506^{*,\#}$
SNX + Q + S ($n = 8$/group)	$804 \pm 152^{*,\&}$	50 ± 11	$496 \pm 29^{\#,\&,\$,\S}$	56 ± 10	$173 \pm 12^{\#}$	$663 \pm 195^{\#}$
SNX + HRH ($n = 8$/group)	950 ± 165	62 ± 19	$905 \pm 160^{*,\#}$	49 ± 12	$173 \pm 31^{\#}$	$914 \pm 223^{*,\#}$
ANOVA	$P < 0.0001$	ns.	$P < 0.0001$	ns.	$P < 0.01$	$P < 0.0001$

$^{*}P < 0.05$ versus sham, $^{\#}P < 0.05$ versus SNX, $^{\&}P < 0.05$ versus SNX+S., $^{\$}P < 0.05$ versus SNX+Q, $^{\S}P < 0.05$ versus SNX+HRH.
Q, quinapril; S, spironolactone; HRH, hydrochlorothiazide+reserpin+hydralazine.
Data as mean ± SD.

Downloaded from ndt.oxfordjournals.org at Semmelweis University Medicine on April 15, 2011

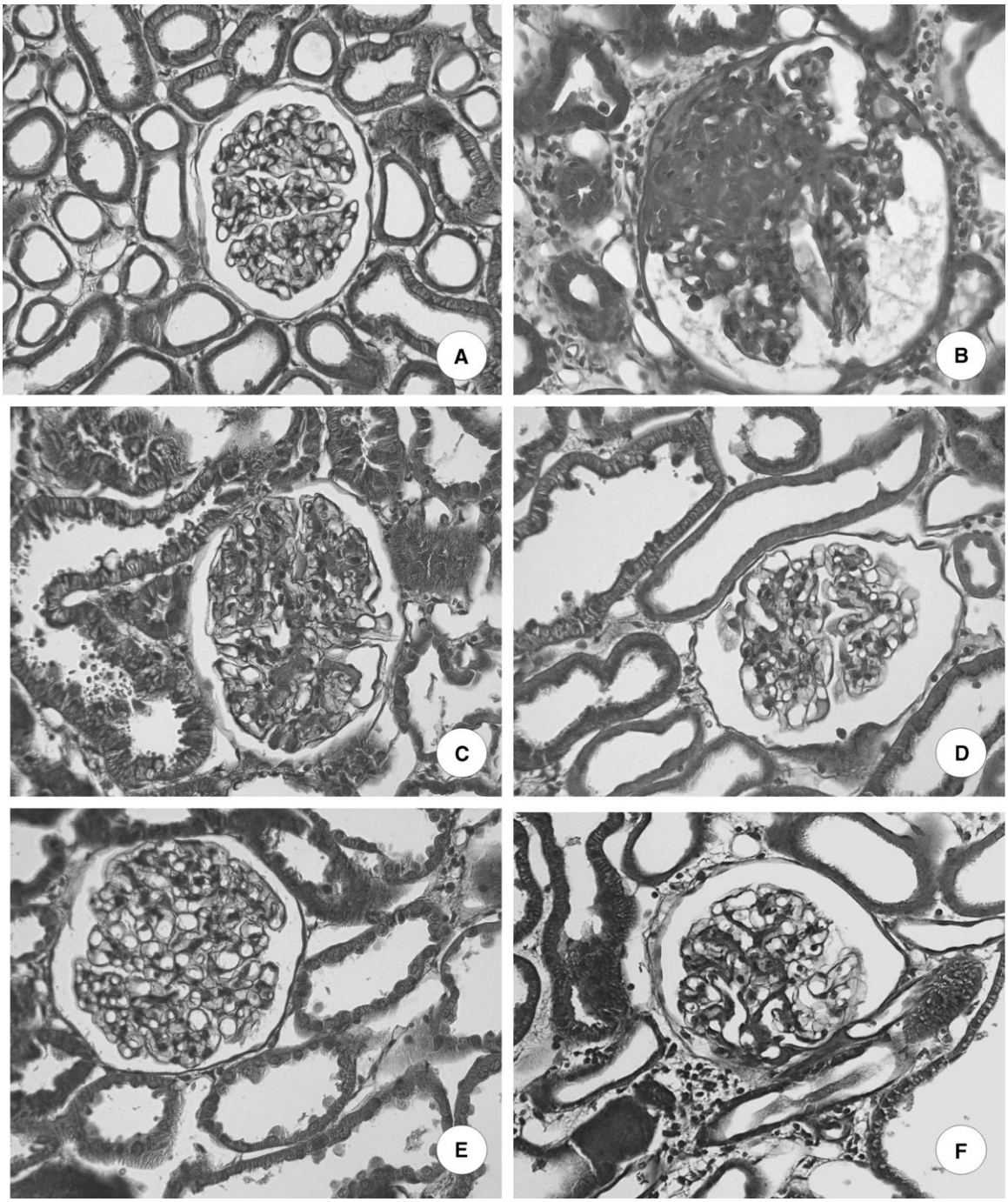

Fig. 1. Glomerular damage indices. (**A**) sham; (**B**) SNX; (**C**) SNX+Q; (**D**) SNX+S; (**E**) SNX+Q+S; (**F**) SNX+HRH. PAS staining, 200× magnification.

intense in the quinapril and spironolactone groups, but was significantly inhibited only in the anti-RAAS combination treatment group.

Similarly, both glomerular and tubulointerstitial extracellular *fibronectin* deposition were significantly elevated in SNX animals compared to sham. Anti-RAAS combination treatment (Q+S) and Q monotherapy, but not spironolactone monotherapy or HRH, reduced the intensity of fibronectin staining.

TGF-β_1 protein staining (Figure 4) was reduced significantly only by quinapril and the anti-RAAS combination treatment Q+S and HRH. In the tubulointerstitial space, only the combination tretament Q+S was able to reduce TGF-β_1 staining. Spironolactone alone was ineffective in both compartments.

Accompanying deposition of fibrotic matrix, *TGF*-β_1 *mRNA* expression in whole kidney samples (Table 7) was markedly higher in SNX compared to sham. Only

Downloaded from ndt.oxfordjournals.org at Semmelweis University Medicine on April 15, 2011

Table 6. Immunohistochemical results

Groups	Collagen IV		Fibronectin			TGF-β_1	
	Glomeruli	Tubulointerstitium volvo Inter	Glomeruli	Tubulointerstitium volvo Inter	Desmin	Glomeruli	Tubulointerstitium
Sham ($n = 9$/group)	0.36 ± 0.16	0.41 ± 0.19	0.36 ± 0.15	0.36 ± 0.16	0.15 ± 0.08	0.12 ± 0.09	0.21 ± 0.13
SNX ($n = 9$/group)	$2.01 \pm 0.26^{*}$	$1.91 \pm 0.31^{*}$	$1.95 \pm 0.32^{*}$	$1.94 \pm 0.31^{*}$	$2.41 \pm 0.30^{*}$	$1.59 \pm 0.27^{*}$	$1.51 \pm 0.35^{*}$
SNX + Q ($n = 9$/group)	$1.55 \pm 0.21^{*}$	$1.51 \pm 0.17^{*}$	$1.44 \pm 0.31^{*,\#}$	$1.42 \pm 0.26^{*,\#}$	$1.19 \pm 0.30^{*,\#}$	$0.57 \pm 0.16^{*,\#,\&}$	$0.62 \pm 0.22^{*,\#}$
SNX + S ($n = 9$/group)	$1.85 \pm 0.20^{*}$	$1.79 \pm 0.18^{*}$	$1.74 \pm 0.33^{*}$	$1.72 \pm 0.22^{*}$	$1.78 \pm 0.28^{*}$	$1.01 \pm 0.13^{*}$	$1.10 \pm 0.33^{*}$
SNX + Q + S ($n = 9$/group)	$0.77 \pm 0.23^{\&,\#}$	$0.75 \pm 0.14^{\#,\&}$	$0.81 \pm 0.38^{*,\#}$	$0.92 \pm 0.36^{*,\#}$	$0.83 \pm 0.29^{*,\#}$	$0.39 \pm 0.20^{\#,\&}$	$0.41 \pm 0.24^{\#}$
SNX + HRH ($n = 9$/group)	nd	nd	$1.72 \pm 0.29^{*}$	$1.82 \pm 0.32^{*}$	Nd	$0.69 \pm 0.17^{*,\#,\&}$	$0.77 \pm 0.13^{*,\#}$
Kruskal–Wallis	$P < 0.0001$	$P < 0.0001$	$P < 0.0001$	$P < 0.0001$	$P < 0.0001$	$P < 0.001$	$P < 0.001$

$^{*}P < 0.05$ versus sham, $^{\#}P < 0.05$ versus SNX, $^{\&}P < 0.05$ versus SNX+S, Kruskal-Wallis test.
Q, quinapril; S, spironolactone; HRH, hydrochlorothiazide+reserpin+hydralazine.
Data as mean ± SD.

Table 7. RT-PCR results

Groups	TGF-β_1
Sham ($n = 9$/group)	0.51 ± 0.08
SNX ($n = 9$/group)	$1.12 \pm 0.11^{*}$
SNX + Q ($n = 9$/group)	0.89 ± 0.15
SNX + S ($n = 9$/group)	$1.04 \pm 0.19^{*}$
SNX + Q + S ($n = 9$/group)	$0.57 \pm 0.29^{\#}$
SNX + HRH ($n = 9$/group)	nd
Kruskal–Wallis	$P < 0.0001$

$^{*}P < 0.05$ versus sham, $^{\#}P < 0.05$ versus SNX, Kruskal-Wallis test.
Q, quinapril; S, spironolactone; HRH, hydrochlorothiazide+reserpin+hydralazine.
Data as mean (mean expression relative to GAPDH) ± SD.

anti-RAAS combination treatment reduces TGF-β_1 mRNA expression significantly.

Discussion

This study in subtotally nephrectomized rats documents that despite similar blood pressure reduction, the combination of a mineralocorticoid receptor blocker and an ACE inhibitor caused more pronounced reduction of albuminuria compared to ACE inhibitor alone or antihypertensive triple therapy. In the background, combination therapy offered significantly better protection of podocytes.

Although blood pressure control by antihypertensive triple therapy without specific effects on the RAS reduced renal function impairment, monotherapies targeting the RAAS system were more effective, similarly to the well-established theory of superior renoprotection of RAAS inhibition over non-specific antihypertensive therapy [32,33].

Monotherapy with the mineralocorticoid receptor blocker caused some reduction of albuminuria and had a beneficial effect on podocyte number and volume, but the effect was less pronounced compared with that of ACE inhibition.

Because the anti-albuminuric effect of combination treatment with ACE inhibition and mineralocorticoid receptor blockade was more pronounced than that of the respective monotherapies, it is of note that the combination was associated with significantly less reduction of podocyte numbers, podocyte volume, podocyte damage and desmin staining.

Green *et al.* [15] were the first to study in the renal ablation model the renoprotective effect of spironolactone at high doses in monotherapy.

The present finding that addition of low doses of spironolactone to RAS blockade provides superior protection in the renal ablation model complements previous studies on the effect of such combination therapy in different renal damage models, such as the THY1-glomerulonephritis [19], the Adriamycin nephrotic syndrome [20] and diabetic nephropathy [21,34,35]. The present study confirms these findings in a non-inflammatory renal damage model and extends the data by providing information on glomerular, interstitial and vascular damage indices, detailed immunohistochemical analysis as well as morphometric analysis of glomeruli and podocytes, specifically documenting less podocyte lesions.

The interest in additional mineralocorticoid receptor blockade in proteinuric patients with RAS blockade started with an observation on eight patients with proteinuria of different aetiologies who were already treated with an ACE inhibitor; the authors found that addition of a low-dose (25 mg/day) spironolactone caused dramatic lowering of proteinuria within 4 weeks [17], which was not explained by changes of blood pressure.

More recently, it has been reported (18) on patients with non-diabetic nephropathy and heavy proteinuria who were treated with an ACE inhibitor plus an angiotensin receptor blocker that they did not respond sufficiently to such dual blockade. Addition of spironolactone (triple blockade) effectively lowered proteinuria without changes in blood pressure. In this observational series, spironolactone was more effective than addition of trichlormethiazide or furosemide.

Since progressive fibrosis is a key factor in progression of kidney damage, it is of interest that aldosterone has previously been shown to reduce progressive fibrosis at least in part by reducing oxidative stress and ANG II independent activation of NF-kappa-B [11,12].

Piecha *et al.* [36] have demonstrated a reversal of glomerulosclerosis by a very high dose of losartan

Downloaded from ndt.oxfordjournals.org at Semmelweis University Medicine on April 15, 2011

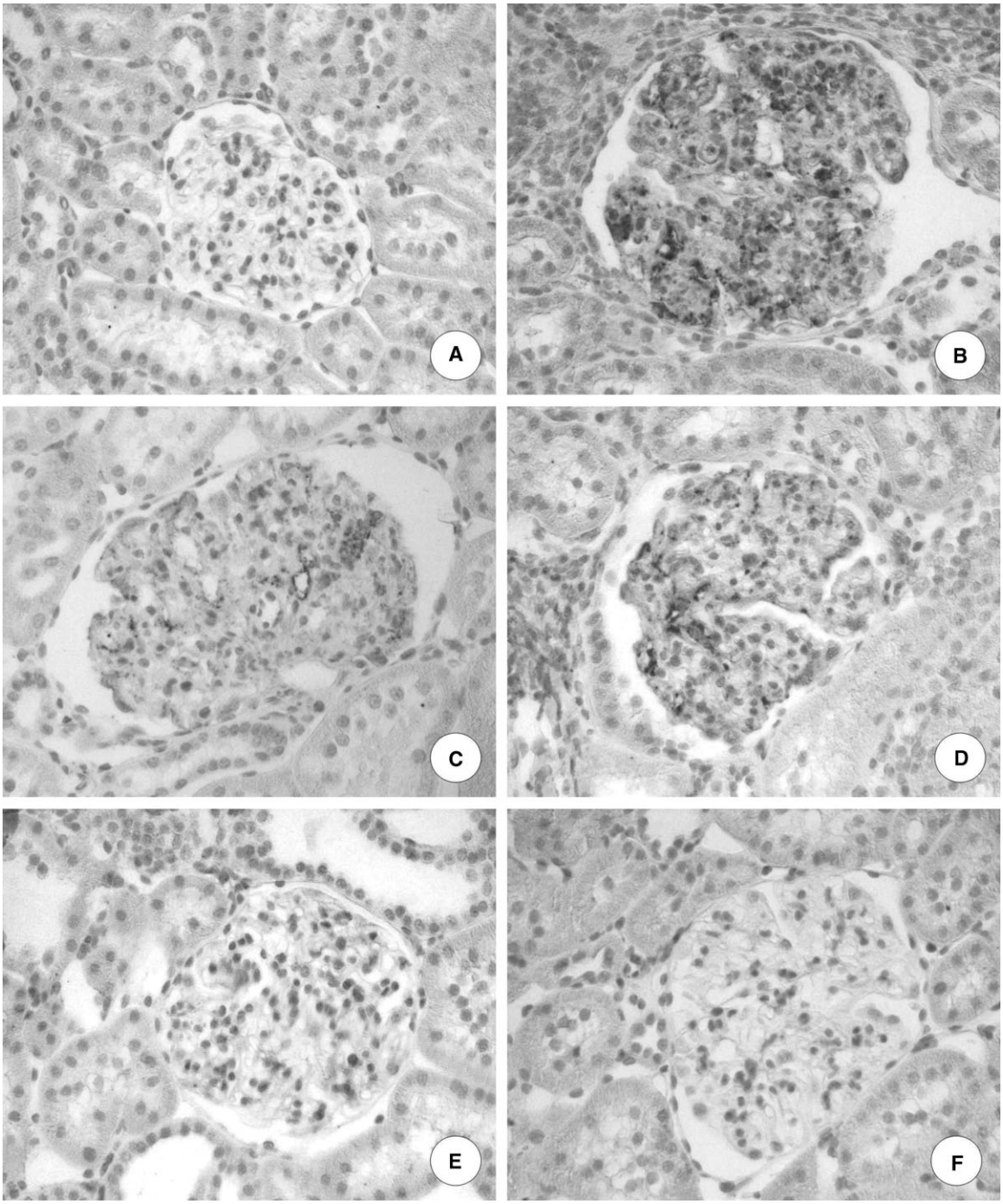

Fig. 2. Immunohistochemical staining of desmin. (**A**) sham; (**B**) SNX; (**C**) SNX+Q; (**D**) SNX+S; (**E**) SNX+Q+S; (**F**) negative control. 200× magnification.

(250 mg/kg body weight/day), and found no further advantage of combination with spironolactone, when a 4-week treatment was initiated 8 weeks after induction of renal fibrosis. The reversal of glomerulosclerosis was explained by the reduction of NFkB signalling and consequent elimination of TGF-beta upregulation and preservation of VEGF production. Our present study further investigated the involvement of double RAAS blockade in the SNX model and demonstrates that progression was better inhibited with combination therapy if initiated early after renal damage. In the background, we found a significantly better protection of podocyte number and damage by 12 weeks of continuous double treatment with pharmacological doses of RAAS inhibition initiated right after SNX versus monotherapies.

Although higher doses of quinapril compared with the usual pharmacologic application of the drug [37], and slightly supra-pharmacologic (2–10× higher) doses of

Downloaded from ndt.oxfordjournals.org at Semmelweis University Medicine on April 15, 2011

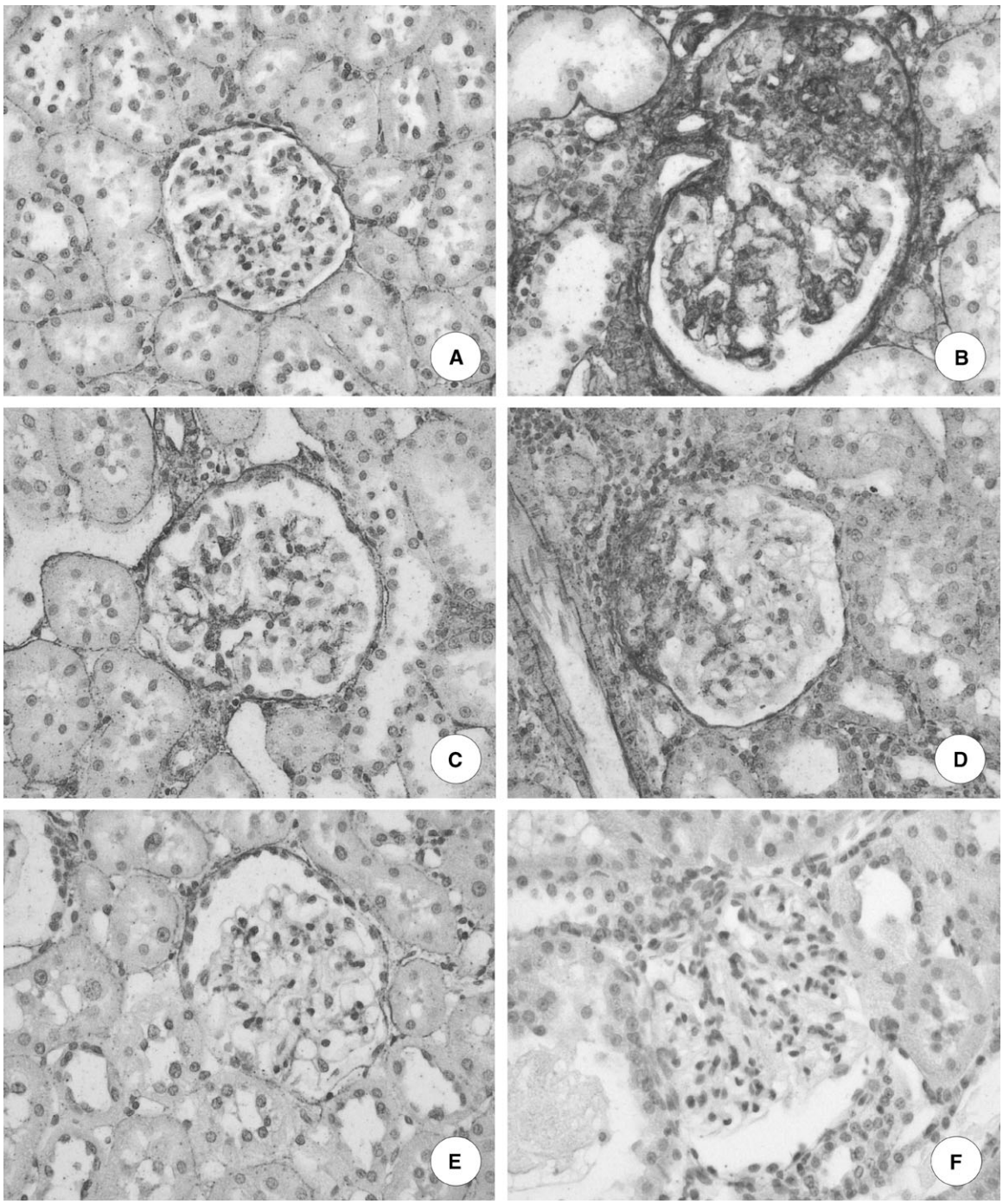

Fig. 3. Immunohistochemical staining of collagen IV. (**A**) sham; (**B**) SNX; (**C**) SNX+Q; (**D**) SNX+S; (**E**) SNX+Q+S; (**F**): negative control. 200× magnification.

spironolactone (10 mg/kg /rat/ versus 1–5 mg/kg /human/[38]) were used in the present study, we did not observe any extra-RAAS effects by the applied doses. These doses applied in the present study were established in a dose adjustment pilot study. Even with much higher doses of quinapril (100 mg/kg), spironolactone (80 mg/kg) and combination, plasma potassium levels were normal (4–5 mmol/l) in all rats. However, high doses of spironolactone caused severe polyuria and dehydration of the rats.

Addition of mineralocorticoid receptor blockers to ACE inhibitors or ARB raises safety issues when used in renal patients. We emphasize that particularly because we had elected for a low dose of spironolactone and extended the observation period to 3 months. In the experiment of Greene [15], the dose of spironolactone was 40-fold higher than in the present study, and no effect was seen after 4 weeks on the glomerulosclerosis index. Using sensitive morphometric methods, we could document significantly less

Downloaded from ndt.oxfordjournals.org at Semmelweis University Medicine on April 15, 2011

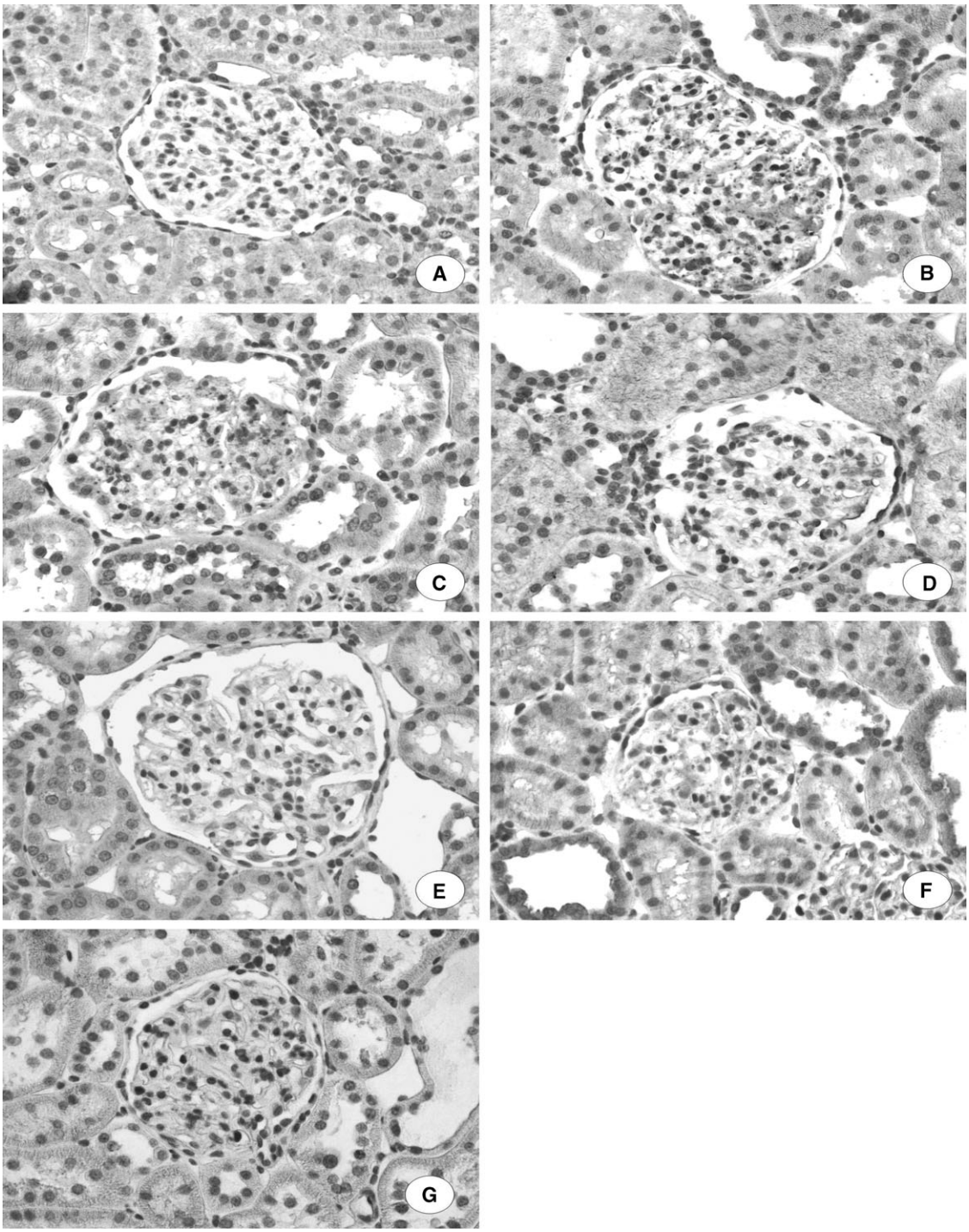

Fig. 4. Immunohistochemical staining of TGF-beta1. (**A**) sham; (**B**) SNX; (**C**) SNX+Q; (**D**) SNX+S; (**E**) SNX+Q+S; (**F**) SNX+HRH; (**G**) negative control. 200× magnification.

mesenchymal matrix expansion even after low dose monotherapy with the mineralocorticoid receptor blocker.

We conclude that in the renal ablation model, the combination of mineralocorticoid receptor blockade on top of ACE inhibition casued a more pronounced decrease of albuminuria and podocyte damage as compared to the respective monotherapies or non-specific antihypertensive triple-therapy.

Our data document that in the renal ablation model, treatment with mineralocorticoid receptor blocker on top of ACE inhibitor caused blood pressure-independent reduction of glomerular damage, particularly podocyte abnormalities, as well as tubulointerstitial injury.

If the data can be translated to humans, these observations could provide a rationale to add spironolactone to the medication of patients with progressive renal disease who

Downloaded from ndt.oxfordjournals.org at Semmelweis University Medicine on April 15, 2011

are unresponsive to or have escaped from RAS blockade. However, the safety of this procedure in humans requires further study.

Acknowledgements. Support was provided to P. H. from the Hungarian Research Fund: OTKA NF69278, T049022, from the Else Kröner Stiftung to L. G. and P. H. and the Intergovernmental Collaboration Program between Hungary (OMFB-TET/D-36) and Germany (DAAD-324 PPP). G. K. received the Hungarian State Eotvos scholarship (No. 41/2006). This research has been supported by DFG (KFG 106, TP6), and the Faculty of Medicine, University of Heidelberg. The skilful technical assistance of H. Ziebart, P. Rieger, Z. Antoni, and M. Weckbach is gratefully acknowledged.

Conflict of interest statement. None declared.

Supplementary data

Supplementary data are available online at http://ndt.oxfordjournals.org.

References

1. Rennke HG, Klein PS. Pathogenesis and significance of nonprimary focal and segmental glomerulosclerosis. *Am J Kidney Dis* 1989; 13: 443–456
2. Hostetter TH, Olson JL, Rennke HG, *et al*. Hyperfiltration in remnant nephrons: a potentially adverse response to renal ablation. *J Am Soc Nephrol* 2001; 12: 1315–1325
3. Wolf G, Butzmann U, Wenzel UO. The renin–angiotensin system and progression of renal disease: from hemodynamics to cell biology. *Nephron Physiol* 2003; 93: P3–P13
4. Wolf G, Ritz E. Combination therapy with ACE inhibitors and angiotensin II receptor blockers to halt progression of chronic renal disease: pathophysiology and indications. *Kidney Int* 2005; 67: 799–812
5. Seikaly MG, Arant BS, Seney FD. Endogenous angiotensin concentrations in specific intrarenal fluid compartments of the rat. *J Clin Invest* 1990; 86: 1352–1357
6. Harris RC, Cheng HF. The intrarenal renin–angiotensin system: a paracrine system for the local control of renal function separate from the systemic axis. *Exp Nephrol* 1996; 4(Suppl 1): 2–7
7. Nishiyama A, Seth DM, Navar LG. Renal interstitial fluid concentrations of angiotensins I and II in anesthetized rats. *Hypertension* 2002; 39: 129–134
8. Huang XR, Chen WY, Truong LD *et al*. Chymase is upregulated in diabetic nephropathy: implications for an alternative pathway of angiotensin II-mediated diabetic renal and vascular disease. *J Am Soc Nephrol* 2003; 14: 1738–1747
9. Richer C, Bruneval P, Menard J *et al*. Additive effects of enalapril and losartan in (mREN-2)27 transgenic rats. *Hypertension* 1998; 31: 692–698
10. Lakkis J, Lu WX, Weir MR. RAAS escape: a real clinical entity that may be important in the progression of cardiovascular and renal disease. *Curr Hypertens Rep* 2003; 5: 408–417
11. Epstein M. Aldosterone as a mediator of progressive renal disease: pathogenetic and clinical implications. *Am J Kidney Dis* 2001; 37: 677–688
12. Juknevicius I, Segal Y, Kren S *et al*. Effect of aldosterone on renal transforming growth factor-beta. *Am J Physiol Renal Physiol* 2004; 286: F1059–F1062
13. Brown NJ, Nakamura S, Ma L *et al*. Aldosterone modulates plasminogen activator inhibitor-1 and glomerulosclerosis *in vivo*. *Kidney Int* 2000; 58: 1219–1227
14. Wakisaka M, Spiro MJ, Spiro RG. Synthesis of type VI collagen by cultured glomerular cells and comparison of its regulation by glucose and other factors with that of type IV collagen. *Diabetes* 1994; 43: 95–103
15. Greene EL, Kren S, Hostetter TH. Role of aldosterone in the remnant kidney model in the rat. *J Clin Invest* 1996; 98: 1063–1068
16. Zoja C, Corna D, Camozzi D *et al*. How to fully protect the kidney in a severe model of progressive nephropathy: a multidrug approach. *J Am Soc Nephrol* 2002; 13: 2898–2908
17. Chrysostomou A, Becker G. Spironolactone in addition to ACE inhibition to reduce proteinuria in patients with chronic renal disease. *N Engl J Med* 2001; 345: 925–926
18. Furumatsu Y, Nagasawa Y, Tomida K *et al*. Effect of renin–angiotensin–aldosterone system triple blockade on non-diabetic renal disease: addition of an aldosterone blocker, spironolactone, to combination treatment with an angiotensin-converting enzyme inhibitor and angiotensin II receptor blocker. *Hypertens Res* 2008; 31: 59–67
19. Asai M, Monkawa T, Marumo T *et al*. Spironolactone in combination with cilazapril ameliorates proteinuria and renal interstitial fibrosis in rats with anti-Thy-1 irreversible nephritis. *Hypertens Res* 2004; 27: 971–978
20. Van Der Meulen EF, Kramer AB, Navis G. Protective effect of combining ACE inhibition and aldosterone receptor blockade on renal structural damage in experimental nephrosis. *J Am Soc Nephrol* 2005; 16: F-PO437
21. Kang YS, Ko GJ, Lee MH *et al*. Effect of eplerenone, enalapril and their combination treatment on diabetic nephropathy in type II diabetic rats. *Nephrol Dial Transplant* 2009; 24: 73–84
22. Amann K, Irzyniec T, Mall G *et al*. The effect of enalapril on glomerular growth and glomerular lesions after subtotal nephrectomy in the rat: a stereological analysis. *J Hypertens* 1993; 11: 969–975
23. Pfeffer JM, Pfeffer MA, Frohlich ED. Validity of an indirect tail-cuff method for determining systolic arterial pressure in unanesthetized normotensive and spontaneously hypertensive rats. *J Lab Clin Med* 1971; 78: 957–962
24. Magnotti RA Jr, Stephens GW, Rogers RK *et al*. Microplate measurement of urinary albumin and creatinine. *Clin Chem* 1989; 35: 1371–1375.
25. Adamczak M, Gross ML, Krtil J *et al*. Reversal of glomerulosclerosis after high-dose enalapril treatment in subtotally nephrectomized rats. *J Am Soc Nephrol* 2003; 14: 2833–2842
26. el Nahas AM, Zoob SN, Evans DJ *et al*. Chronic renal failure after nephrotoxic nephritis in rats: contributions to progression. *Kidney Int* 1987; 32: 173–180
27. Véniant M, Heudes D, Clozel JP *et al*. Calcium blockade versus ACE inhibition in clipped and unclipped kidneys of 2K-1C rats. *Kidney Int* 1994; 46: 421–429
28. Schwarz U, Amann K, Orth SR *et al*. Effect of 1,25 (OH)2 vitamin D3 on glomerulosclerosis in subtotally nephrectomized rats. *Kidney Int* 1998; 53: 1696–1705
29. Amann K, Nichols C, Tornig J *et al*. Effect of ramipril, nifedipine, and moxonidine on glomerular morphology and podocyte structure in experimental renal failure. *Nephrol Dial Transplant* 1996; 11: 1003–1011
30. Buzello M, Haas CS, Hauptmann F *et al*. No aggravation of renal injury in apolipoprotein E knockout mice (ApoE(−/−)) after subtotal nephrectomy. *Nephrol Dial Transplant* 2004; 19: 566–573
31. Gross ML, El-Shakmak A, Szabo A *et al*. ACE-inhibitors but not endothelin receptor blockers prevent podocyte loss in early diabetic nephropathy. *Diabetologia* 2003; 46: 856–868
32. Raij L, Chiou XC, Owens R *et al*. Therapeutic implications of hypertension-induced glomerular injury. Comparison of enalapril and a combination of hydralazine, reserpine, and hydrochlorothiazide in an experimental model. *Am J Med* 1985; 79: 37–41
33. Anderson S, Rennke HG, Brenner BM. Therapeutic advantage of converting enzyme inhibitors in arresting progressive renal disease associated with systemic hypertension in the rat. *J Clin Invest* 1986; 77: 1993–2000.
34. Han SY, Kim CH, Kim HS *et al*. Spironolactone prevents diabetic nephropathy through an anti-inflammatory mechanism in type 2 diabetic rats. *J Am Soc Nephrol* 2006; 17: 1362–1372

Downloaded from ndt.oxfordjournals.org at Semmelweis University Medicine on April 15, 2011

35. Han KH, Kang YS, Han SY *et al*. Spironolactone ameliorates renal injury and connective tissue growth factor expression in type II diabetic rats. *Kidney Int* 2006; 70: 111–120
36. Piecha G, Koleganova N, Gross ML *et al*. Regression of glomerulosclerosis in subtotally nephrectomized rats: effects of monotherapy with losartan, spironolactone, and their combination. *Am J Physiol Renal Physiol* 2008; 295: F137–F144
37. Mokwe E, Ohmit SE, Nasser SA *et al*. Determinants of blood pressure response to quinapril in black and white hypertensive patients: the quinapril Titration Interval Management Evaluation trial. *Hypertension* 2004; 43: 1202–1207
38. Struthers A, Krum H, Williams GH. A comparison of the aldosterone-blocking agents eplerenone and spironolactone. *Clin Cardiol* 2008; 31: 153–158

Received for publication: 9.2.09; Accepted in revised form: 6.7.09

Nephrol Dial Transplant (2009) 24: 3651–3658
doi: 10.1093/ndt/gfp407
Advance Access publication 7 August 2009

Azelnidipine exerts renoprotective effects by improvement of renal microcirculation in angiotensin II infusion rats

Sohachi Fujimoto, Minoru Satoh, Hajime Nagasu, Hideyuki Horike, Tamaki Sasaki and Naoki Kashihara

Division of Nephrology, Department of Internal Medicine, Kawasaki Medical School, Kurashiki, Okayama, Japan

Correspondence and offprint requests to: Minoru Satoh; E-mail: msatoh@med.kawasaki-m.ac.jp

Abstract

Background. Hypoxia-induced tubulointerstitial injury caused by loss of peritubular capillary (PTC) blood flow may be associated with progressive renal disease. Therefore, the maintenance of blood flow in PTCs may protect against loss of renal function. A long-acting calcium channel blocker, azelnidipine, has been shown to be useful in the treatment of progressive renal disease. However, its mechanism of action remains unclear. The aim of the present study was to elucidate whether azelnidipine maintains PTC blood flow and to compare it to nifedipine in its ability to improve tubulointerstitial injury caused by angiotensin II (AII) infusion in rats.

Methods. PTC blood flow was initially monitored using a pencil-lens interval microscope before and after intravenous AII (30 ng/kg/min) infusion with or without azelnidipine (10 μg/kg/min). Next, Wistar rats were treated with chronic infusion of AII (500 ng/kg/min) via an osmotic minipump with or without azelnidipine (3 mg/kg/day, orally) or nifedipine (60 mg/kg/day, orally) for 14 days, and tubulointerstitial damage (PTC loss, interstitial fibrosis, tubular atrophy) was examined.

Results. PTC blood flow was reduced after AII infusion but improved after a bolus injection of azelnidipine. Tubulointerstitial damage observed in chronically AII-treated kidneys was associated with hypoxic conditions, as indicated by the measurement of hypoxia biomarkers (intracellular hypoxyprobe-1 adducts). These tubulointerstitial injuries in AII-infused rats were more effectively reduced by azelnidipine than by nifedipine. The area showing hypoxic conditions in the kidney was also more reduced with azelnidipine than nifedipine treatment.

Conclusions. Azelnidipine may increase PTC blood flow and improve renal hypoxia and tubulointerstitial injury induced by AII infusion.

Keywords: calcium channel blocker; hypoxia; peritubular capillary; tubulointerstitial injury

Introduction

Tubulointerstitial injury is an important risk factor for progressive renal damage [1,2]. It is reported that ischaemia, i.e. a decrease in tissue oxygen concentration caused by loss of peritubular capillaries (PTCs) and a decrease in blood flow in PTCs, is extensively involved in the pathogenesis of tubulointerstitial injury [3–5]. Therefore, the maintenance of blood flow in PTCs and the resultant improvement of tissue hypoxia may prevent progression of renal damage.

Calcium channel blockers (CCBs) are the most commonly used antihypertensive agents. Their renoprotective effects have been demonstrated in many studies using experimental models of renal damage, especially those of hypertensive renal damage [6–8]. Recent large-scale clinical studies, such as the Lipid-Lowering Treatment to Prevent Heart Attack Trial and international Nifedipine GITS study: Intervention as a Goal in Hypertension Treatment, have shown that long-acting dihydropyridine CCBs effectively suppress progression of renal damage [9,10]. Several hypotheses have been proposed for the mechanism of such renoprotective effects of CCBs; one of these proposed mechanisms is the improvement of renal haemodynamics

© The Author 2009. Published by Oxford University Press [on behalf of ERA-EDTA]. All rights reserved.
For Permissions, please e-mail: journals.permissions@oxfordjournals.org

Downloaded from ndt.oxfordjournals.org at Semmelweis University Medicine on April 15, 2011